J Membrane Biol (2008) 226:17–25
DOI 10.1007/s00232-008-9135-3

Stretch-Activated Potassium Channels in Hypotonically Induced Blebs of Atrial Myocytes

Xuxia Liu · Haixia Huang · Wei Wang · Jun Wang · Frederick Sachs · Weizhen Niu

Received: 5 September 2008 / Accepted: 8 October 2008 / Published online: 18 November 2008

Abstract Stress in the lipids of the cell membrane may be responsible for activating stretch-activated channels (SACs) in nonspecialized sensory cells such as cardiac myocytes, where they are likely to play a role in cardiac mechanoelectric feedback. We examined the influence of the mechanical microenvironment on the gating of stretch-activated potassium channels (SAKCs) in rat atrial myocytes. The goal was to examine the role of the cytoskeleton in the gating process. We recorded from blebs that have minimal cytoskeleton and cells treated with cytochalasin B (cyto-B) to disrupt filamentous actin. Histochemical and electron microscopic techniques confirmed that the bleb membrane was largely free of F-actin. Channel currents showed mechanosensitivity and potassium selectivity and were activated by low pH and arachidonic acid, similar to properties of TREK-1. Some patches showed a time-dependent decrease in current that may be adaptation or inactivation, and since this decrease appeared in control cells and blebs, it is probably not the result of adaptation in the cytoskeleton. Cyto-B treatment and blebbing caused an increase in background channel activity, suggesting a transfer of stress from actin to bilayer and then to the channel. The slope sensitivity of gating before and after cyto-B treatment was similar to that of blebs, implying the characteristic change of dimensions associated with channel gating was the same in the three mechanical environments. The mechanosensitivity of SAKCs appears to be the result of interaction with membrane lipids and not of direct involvement of the cytoskeleton.

Keywords Stretch-activated channel · TREK · Cytochalasin B · Cytoskeleton · Mechanoelectric feedback · Costamere · Actin · Bleb

X. Liu · H. Huang · W. Wang · J. Wang · W. Niu (✉)
Department of Physiology, Capital Medical University, Beijing 100069, People's Republic of China
e-mail: niuwz@126.com

X. Liu
e-mail: lxxlskjnet@gmail.com

F. Sachs
Department of Physiology and Biophysical Sciences, State University of New York at Buffalo, Buffalo, NY 14214, USA

Introduction

Mechanical stress affects the electrical activity of the heart; this effect is noted as mechanoelectric feedback (MEF). MEF can be classified into three categories. First, chronic cardiac overload induces electrical remodeling by changing gene expression for various channels and transporters. The process may begin within several minutes (Yamazaki et al. 1996) and continues as long as the overload exists. Second, cardiac overload can influence cardiac electric activity via various chemical signals, such as NO, Ca^{2+}, G proteins, PIP_2 and DG, within seconds or minutes (Casadei and Sears 2003). The third type occurs within milliseconds. Franz et al. (1992) showed that in the perfused rabbit heart step-like changes in ventricular volume could pace the heart. Similarly, steps in ventricular pressure may induce a premature beat (Wei et al. 2006). Because the electric responses can take place in less than 100 ms following a mechanical interference, the third type of MEF is thought to be caused directly by the activation of stretch-activated channels (SACs). To distinguish this process from the other two, we refer to this MEF as "fast MEF."

SACs are found in all cells including muscle, epithelium and osteoblasts. Three types of SAC currents in the heart have been reported (Hu and Sachs 1997): cation-selective, K^+-selective and volume-activated $C1^-$ currents (Baumgarten and Clemo 2003). Several members of the transient receptor potential (TRP) and two-pore domain K^+-channel superfamily and epithelial Na^+ channels are candidates for SACs in eukaryotic cells (Martinac 2004), and the protein identity for SAC currents in eukaryotes is still unsettled (Gottlieb et al. 2008).

There are two basic models for SAC activation: cytoskeletal tethering and bilayer stress (Christensen and Corey 2007; Hamill 2006; Hamill and McBride 1997; Martinac 2004; Zhang et al. 2000). In the tethered model, SAC stress is transferred to the channel directly through fibrous proteins. For example, in hair cells of the inner ear force is transmitted to SACs via the tip link, an extracellular filament (Corey 2003; Corey and Hudspeth 1983). The influence of the cytoskeleton in activation of SAC in oocytes was suggested in a study in which adaptation and mechanosensitivity were lost after repeated mechanical stimulation (Hamill 2006; Hamill and McBride 1992). The bilayer model was proven with reconstituted mechanosensitive channels of small conductance or large conductance (MscS or MscL) from the inner membrane of *Escherichia coli* (Martinac 2004; Martinac et al. 1990; Sukharev 2002; Sukharev et al. 1994). The same gating mechanism was suggested in a study on the SAC of the *Xenopus* oocyte (Zhang et al. 2000), which was reported to be TRPC-1 (Maroto et al. 2005).

TREK-1 is a stretch-activated K^+ channel (SAKC) belonging to the two-pore domain K^+-channel (K_{2P}) superfamily. It is also activated by intracellular acidity and various amphipaths, such as arachidonic acid (AA) (Maingret et al. 1999), and is expressed in cardiac myocytes (Tan et al. 2002; Terrenoire et al. 2001; Xian Tao et al. 2006) and the nervous system (Lesage and Lazdunski 2000; Patel et al. 2001). Several lines of evidence suggest that TREK-1 is activated via bilayer stress when expressed in *Xenopus* oocytes and other cell lines (Honore et al. 2006; Lopes et al. 2005; Patel et al. 2001). TREK-1 activity is increased after disrupting F-actin (Patel et al. 2001) and affected by amphipaths, suggesting bilayer stress can play a role (Patel et al. 2001). The carboxy-terminal positively charged cluster (E306) seems to be a PIP_2 receptor that affects mechanical gating (Chemin et al. 2005). Thus, TREK-1 may be activated by force coupled directly through membrane lipids. SAKC currents with TREK-1-like properties have been recorded in cardiac myocytes (Tan et al. 2002; Terrenoire et al. 2001). To further test the idea of lipid gating, we used hypotonically induced blebs (Collins et al. 1992; Hilgemann 1989) that were devoid of cortical F-actin. Cardiac SAKCs can be activated without direct involvement of cortical F-actin.

Materials and Methods

Cell Isolation

Atrial myocytes were enzymatically isolated by retrograde perfusion of the heart. Briefly, Sprague-Dawley rats (female 250–300 g) were injected with heparin (2,500 units/kg) and then with sodium pentobarbital (1 mg/kg). When the rat was anesthetized, the heart was quickly excised and rinsed with 4°C buffer solution. The heart was retrogradely perfused via a Langendorff apparatus with Ca^{2+}-free Tyrode's solution for 5–6 min, then Ca^{2+}-free Tyrode's solution containing 0.05% collagenase (type II; Worthington, Freehold, NJ) and 0.025% BSA (fraction V; Sigma-Aldrich, St. Louis, MO) for 30–40 min. All perfusion solutions were equilibrated with 95% oxygen and 5% CO_2. After collagenase phase, the atria were cut into small pieces, mechanically dissociated into single cells and then stored in KB solution at 4°C. KB solution contained (in mM) KCl, 40.0; KOH, 80.0; KH_2PO_4, 25.0; $MgSO_4$, 3.0; glucose, 10.0; taurine, 20.0; glutamic acid, 50.0; EGTA, 1.0; and HEPES, 10.0 and was adjusted to pH 7.4 with NaOH.

Blebbing Rat Atrial Myocytes and Bleb Morphology

Isolated atrial myocytes were treated in hypotonic solution (64–160 mOsm/L), diluted from a storage solution with the following composition (in mM): KCl, 150.0; HEPES, 15.0; $MgC1_2$, 2.0; EGTA, 10.0; and dextrose, 20.0, adjusted to pH 7.2 with KOH. After incubating these myocytes hypotonically for 30–40 min at room temperature, blebs formed (Fig. 1).

Blebbed myocytes were dropped on a polylysine-coated slide. Alexa Fluor 488 phalloidin (Molecular Probes, Eugene, OR) and $DiIC_{16}$ (Molecular Probes) were added to PBS solution, containing 3.7% formaldehyde, as the staining solution. Blebbed cells were incubated in the staining solution for 30 min at 4°C to label F-actin and lipids and examined with an inverted fluorescent microscope (Diaphot 300; Nikon, Tokyo, Japan). To examine in more detail, cells were imaged via confocal microscopy (LAS AF-SP5; Leica Microsystems, Wetzlar, Germany). Membranes were clearly visible with $DiIC_{16}$ at 0.03 mg/ml. F-actin was stained with Alexa Fluor 488 phalloidin at 3–7 μg/ml.

Cells were examined at higher resolution with electron microscopy (80 kV JEM-1230; JEOL, Tokyo, Japan). Myocytes were fixed in 3% glutaraldehyde for 2 h, post-fixed in 1% OsO_4 for 2 h, gradually dehydrated in ethanol, embedded in Spurr and stained with uranyl acetate and lead citrate.

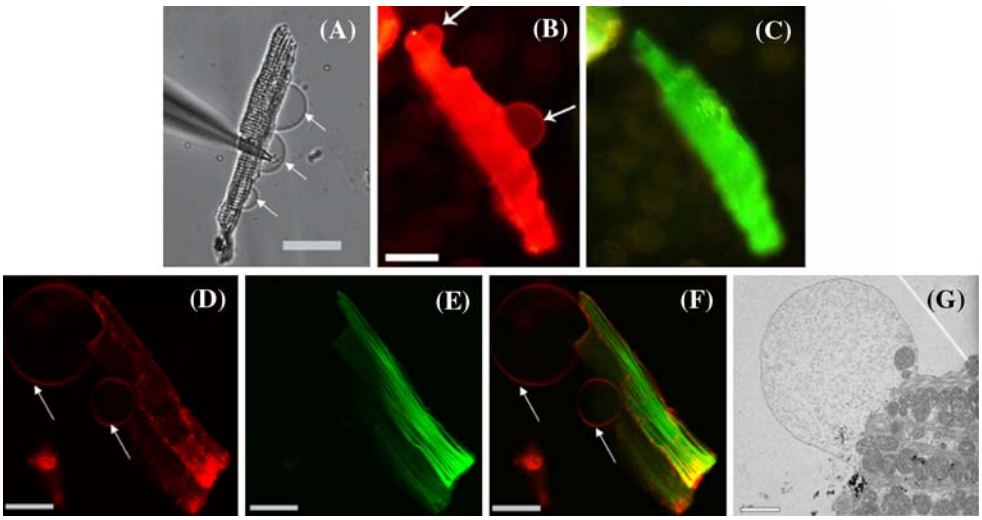

Fig. 1 Morphology of the blebbed atrial myocyte. **a** Phase contrast image of cell with blebs in hypotonic solution. The tip of a pipette was sealed to one bleb. **b, c** Fluorescent images of the same cell with the membrane labeled with $DiIC_{16}$ in red and the actin labeled with phalloidin in green. **d, e** A group of cells under the same visual field of a confocal microscope and merged in (**f**). **g** Electron micrograph of a bleb with a smooth membrane and disordered material inside. No caveoli are visible. Scale bars = 25 μm for (**a–f**) and 2 μm for (**g**)

Single-Channel Recording

SAKC activity was recorded in cell-attached or inside–out configuration at room temperature under three different conditions: control cells, after treatment with cytochalasin B (cyto-B) and after blebbing. We chose blebbed myocytes with clear striations and well-defined margins (Fig. 1). Suction steps were delivered to the pipette with a water-filled manometer in a resolution of 5 mm H_2O with one end open to atmosphere and the other to the pipette via a three-way valve and a 20-ml syringe connected to the valve. The rise time was ~1 s. The patch pipette was made from borosilicate glass (BF150-110-10; Sutter Instrument, Novato, CA) without Sylgard coating or fire-polishing and had resistance of 4.0-6.0 MΩ. The channel current was amplified and filtered at 10 kHz (Axopatch-200A; Axon Instruments, Foster City, CA), digitized at 20 kHz and finally analyzed at 2 kHz, using an acquisition system (Digidata 1322A and pCLAMP 9.2, Axon Instruments).

Data were analyzed with QuB (www.qub.buffalo.edu) and pClamp 9.2 (Axon Instruments). When there was more than one SAKC channel in a patch, which was the usual case, channel activity was expressed as $N \times P_o$ (NP_o) and calculated with the following equation (pClamp manual):

$$NP_o = 1 \times To_1 + 2 \times To_2 + 3 \times To_3 + \cdots + L \times To_L \quad (1 \le L \le N)$$

where N is the number of channels in the patch, P_o the open probability of one single channel, L the level of the channel opening and To_L the open time at level L divided by the total observation time. For each recording, 5-s steady-state currents or 100-ms peak currents were analyzed to obtain NP_o.

Solutions for Patch-Clamp Experiment

The standard pipette solution and bath solution were the same and contained (mM) KCl (or potassium aspartate), 140.0; HEPES, 10.0; $MgCl_2$, 2.0; and EGTA, 5.0, adjusted to pH 7.2 with KOH. The high-Na pipette solution was similar to the standard except that KCl (or potassium aspartate) was replaced with 140 mM NaC1 or sodium gluconate. TEA (5 mM) and glybenclamide (10 μM) were added to the bath solution to block voltage-gated and ATP-sensitive potassium channels, respectively. Stock solutions of AA dissolved in ethanol at a concentration of 100 mM were kept at −20°C and used within 1 week. Cyto-B (20 μM dissolved in 0.1% DMSO) was used to degrade F-actin (Furukawa et al. 1996). Potassium aspartate, sodium gluconate, AA, glybenclamide and cyto-B were all purchased from Sigma-Aldrich.

Reverse Transcription-Polymerase Chain Reaction

Total RNA from the four chambers of the adult rat heart was extracted separately with the RNeasy kit following the manufacturer's protocol (Invitrogen, Carlsbad, CA). Purified RNA was reverse-transcribed into first-strand cDNA using oligo-dT primers and AMV reverse transcriptase (Takara, Otsu, Japan). cDNA products were used as templates for PCR amplification with Taq DNA polymerase (Takara). Control reactions without template RNA were included for each PCR amplification experiment. Gene-specific primers for rat TREK-1 were forward 5′-CTCAG GAGATTTCTCAGAGGACCAC-3′ and reverse 5′-CTAA CATTCCACTTAATAAATGTGTC-3′. Primers for β-actin

were forward 5′-AAGATGACCCAGATCATGTT-3′ and reverse 5′-TTGATGTCACGCACGATTTC-3′. RT-PCR conditions were 2 min at 94°C, followed by 40 cycles of 30 s at 94°C, 30 s at 55°C, 30 s at 72°C and a final extension of 7 min at 72°C. PCR products (expected fragment sizes: TREK-1, 398 bp; β-actin, 287 bp) were analyzed on a 1.5% agarose gel by electrophoresis and visualized with ethidium bromide.

Data Analysis

Data were expressed as mean ± SE. With paired *t*-test, unpaired *t*-test or two-way ANOVA, significance was set at $P < 0.05$.

Results

SAC Microenvironment Without Cortical F-Actin

Figure 1a shows a blebbed atrial myocyte after incubation in hypotonic solution (100 mOsm/L) for 40 min. Three smooth semicircular membrane blebs are seen clearly on the right-hand side of the cell (Fig. 1a). The base of the bleb spanned several sarcomeres, suggesting that the local costameres had been broken.

To investigate whether F-actin remained beneath the bleb membrane, we labeled cellular lipids and F-actin with $DiIC_{16}$ and Alexa Fluor 488 phalloidin, respectively. Figure 1b, c shows the double-labeled fluorescent images. The two clear blebs (arrows) on the surface of the myocytes emit red fluorescence ($DiIC_{16}$) but no green fluorescence (phalloidin). To affirm this result, cells were scanned via confocal microscopy. Figure 1d, e shows scanned images at the same level. Figure 1d shows the bleb membrane (arrow) and sarcolemma of the atrial myocytes. Membrane blebs did not show phalloidin fluorescence. Quantitative analysis of F-actin fluorescence at the location of the bleb membrane showed no significant difference with the background ($P > 0.05$, $n = 6$, data not shown). Electron micrographs of blebs show a smooth membranous structure with amorphous granular material but no organelles within the bleb and no caveoli in the membrane (Fig. 1g).

Comparison of SAKCs in the Control Membrane and Blebs

Identification of SACs in the Sarcolemma of Control Myocytes and Blebs

SACs were identified in the control myocyte and the bleb of the myocyte following the earlier study (Kim et al. 1995; Niu and Sachs 2003), with the addition of TEA (5 mM) and glybenclamide (10 μM) in the bath solution. Figure 2 displays single-channel SAC activity recorded at +40 m*V* on the two kinds of patches in cell-attached configuration. There was spontaneous activity at 0 mm Hg (Fig. 2a). This was more obvious in the bleb patch where a higher tension might have developed during blebbing (Akinlaja and Sachs 1998) (Fig. 2b). When negative pressure (−20 mm Hg) was applied, the channel activated after a short delay (Fig. 2). SAC activity in both types of patches did not run down during repeated long suction pulse (15–20 s/pulse). Channel activity in both types of patch returned to control levels after the release of pressure. Amplitude histograms of 5-s records showed that the unitary conductance was the same before and after stretching in both types of patch (Fig. 2). Out of 233 sealed control myocytes, 67 patches were confirmed to contain SACs, while 28 of 143 sealed blebs had SAC activity. Figure 2b shows obvious adaptation/inactivation in a bleb patch. However, in Fig. 2a, a mild adaptation/inactivation could be recognized by carefully analyzing the NP_o time course (data not shown). Out of 28 bleb patches with SAC activity, 14 (50%) showed obvious adaptation/inactivation (Fig. 2b). For control patches, mild adaptation/inactivation activity could be confirmed in 15/67 SAC patches. The following experiments show the SACs were K-selective.

Identity of SACs in the Control Sarcolemma and Blebs

To characterize the ionic permeability, we used two pipette solutions (high-K^+ or high-Na^+) to make current-voltage (*I–V*) curves with a ramp protocol from +80 to −80 m*V* lasting 40 s (Fig. 3). In control atrial myocytes, the *I–V* curve was linear with a reverse potential of 0 m*V* (Fig. 3a, e) and the single-channel conductance was 56 ± 7 pS ($n = 6$) at +60 m*V*. Substituting Na^+ for K^+ in the pipette saline, the outward current remained but there was no inward current even at −80 m*V* (Fig. 3b, e). Channels in blebs had the same properties (Fig. 3c, d). Currents were not affected by replacing Cl^- with aspartate or gluconate in the pipette solution (Fig. 3c, d). Mean conductance in blebs was similar to that obtained in control atrial myocytes (Fig. 3e). SAC ion permeability in both types of patch membrane appears similar and K^+-selective (SAKC).

The SAKC in rat atrial myocytes has been proposed to be TREK-1. A characteristic signature of TREK-1 is sensitivity to membrane stretch, AA and intracellular acidity (Patel et al. 2001). NP_o of the recorded channels in both kinds of patches increased with suction, AA (10 μM) and intracellular acidification (pH 5.6–7.2) in inside–out mode (Fig. 4a–c); and mRNA for TREK-1 was found in cardiac cells (Fig. 4d). Thus, the SAKCs recorded in control myocytes and blebs may be TREK-1 or a very closely related member of the K_{2P}-channel superfamily.

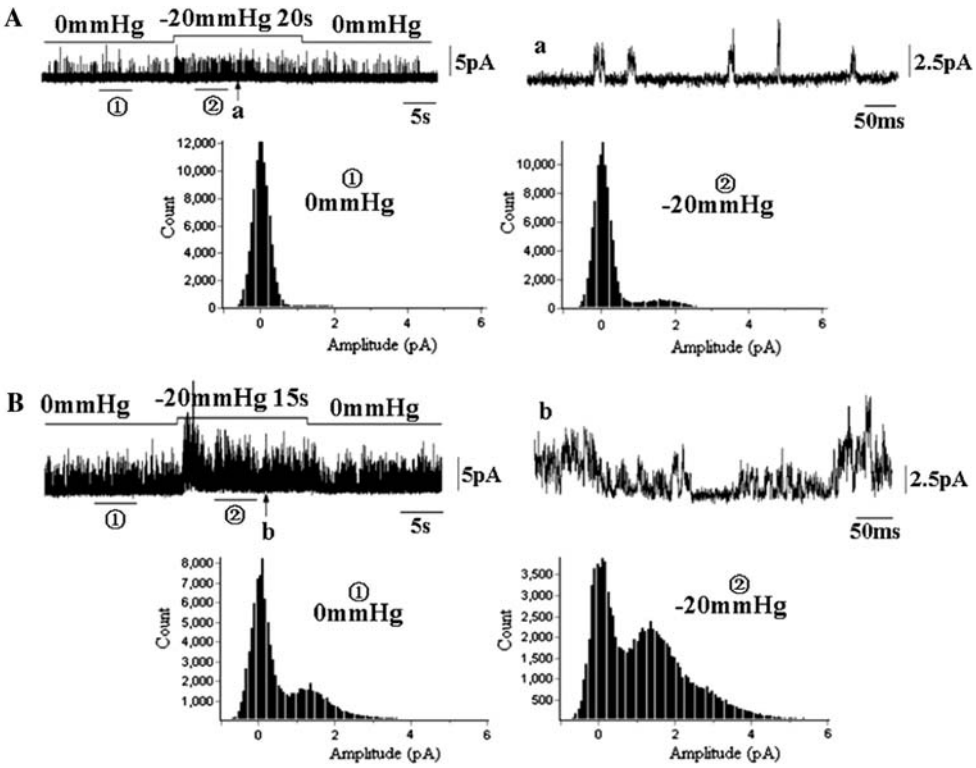

Fig. 2 SAC activity recorded from control membrane (**a**) and blebs (**b**) in cell-attached mode. The patch potential was held at 40 m*V* with the cell in potassium solution (K^+ 140 mM). Channel activity increased with suction (−20 mm Hg). *Right traces* (*a, b*) are shown at a higher time resolution, chosen at the time marked with the corresponding letters in the *left traces*. Outward current is upward. All-points histograms from the recordings in ① and ② show the same current amplitudes before and during suction

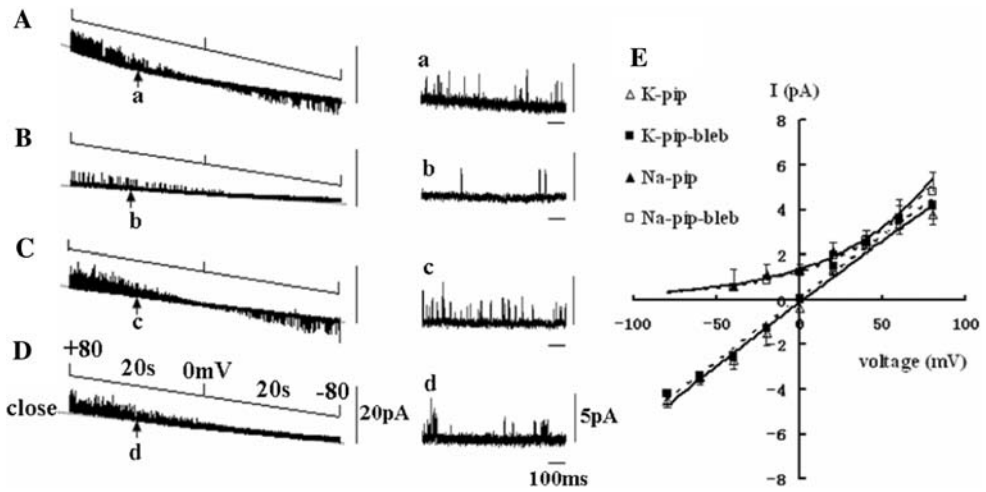

Fig. 3 Ion selectivity and current–potential curve of SACs in the control myocyte and bleb membrane. All channel currents were recorded in cell-attached mode with bath solution containing 140 mM K^+. Potential ramps from +80 to −80 m*V*, the estimated membrane potential, lasted for 40 s. **a** and **b** were from two control atrial myocytes. Inward and outward currents were recorded with a pipette containing 140 mM KCl and 0 mM Na^+ in **a**. However, only outward current could be recorded when the pipette solution was changed to 140 mM NaCl and 0 mM K^+ in **b**. **c** and **d** were recorded on the membrane of two blebs with the pipette solution containing either 140 mM potassium aspartate (**c**) or 140 mM sodium gluconate (**d**). Replacement of 140 mM potassium aspartate (**c**) with 140 mM sodium gluconate (**d**) in the pipette produced only outward current. Traces *a–d* were expanded, chosen at the times tagged on the *left records* with the corresponding letters. **e** *I–V* curves of SACs in the control and bleb membrane with different pipette solutions. Δ and ▲, KCl ($n = 6$) and NaCl ($n = 4$) pipette solution applied in the experiment on control myocytes, respectively; ■ and □, pipette solution of potassium aspartate ($n = 6$) and sodium gluconate ($n = 4$) used on the patches of blebs, respectively

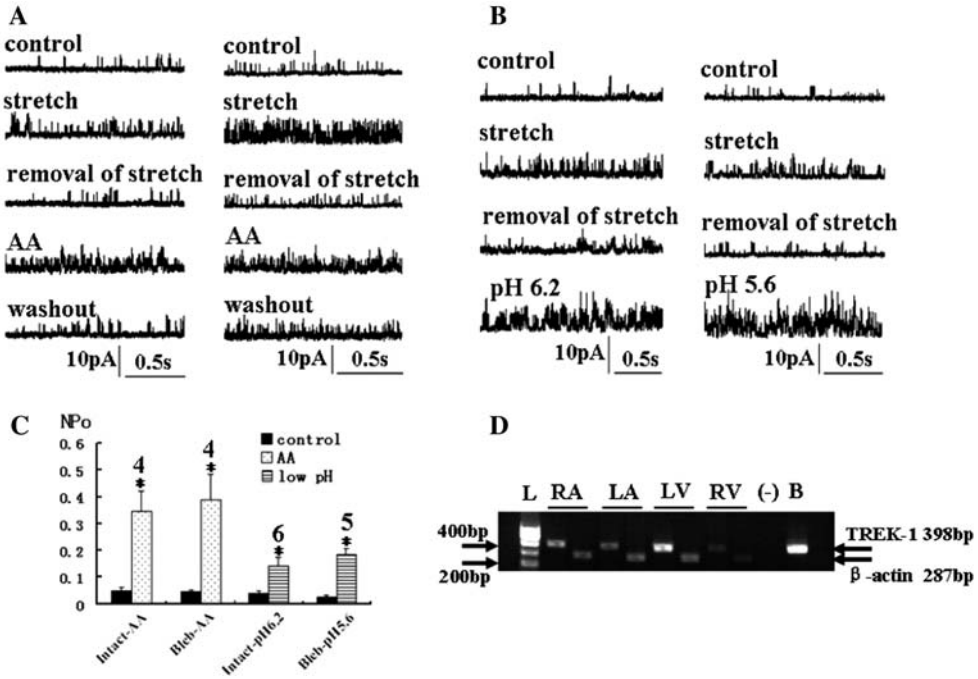

Fig. 4 SAKC responses to AA and low intracellular pH in control myocytes and blebs (**a–c**) and expression of TREK-1 in adult rat heart (**d**). Channel activity was recorded in inside–out configuration at +40 mV in symmetrical K^+ solution. Experiments in **a** and **b** were done in the control cell (*left*) and bleb (*right*). **a** *From the top down*, channel activity was continuously recorded in the conditions of control (0 mm Hg), −20 mm Hg, 0 mm Hg, AA (10 μM) and washout. **b** *From the top down*, channel activity was continuously recorded in the conditions of control (0 mm Hg and pH 7.2), −20 mm Hg, 0 mm Hg and pH 6.2 or 5.6. **c** Statistics of the effect of AA and pH. Intact-AA and Bleb-AA, treatments of the control and bleb patches with AA, respectively; Intact-pH 6.2 and Bleb-pH 5.6, treatments of the control and bleb patches with low pH, respectively. Numbers on each bar indicate the number of different patches. Asterisks indicate statistical significance ($^*P < 0.05$). **d** TREK-1 and β-actin amplification by RT-PCR from the left atrium (LA), right atrium (RA), left ventricle (LV) and right ventricle (RV). RNA (–) was a negative control for TREK-1. RT-PCR of the brain (B) is a positive control. The molecular ladders (L) are shown on the *left*. The predicted size is 398 bp for TREK-1 and 287 bp for β-actin

Mechanosensitivity of SAKCs in Different Mechanical Microenvironments

The above results suggest that SAKC gating is driven by stress in the membrane, not the cytoskeleton. To check further, we compared SAKC activity in myocytes before and after treatment with cyto-B and in blebs. Figure 5a, b records sarcolemma of the same myocyte before and after treatment with cyto-B, and Fig. 5c is from the bleb membrane of another myocyte. Graded mechanical stimulation from 0 to −40 mm Hg could not usually reach saturation because of patch fragility, especially in blebs; but gating was stimulus-dependent in the three situations. The relationship between NP_o and suction could be fitted by $NP_o = Ae^{kx}$, where x is the pressure, A is the background activity and k reflects the sensitivity in units of 1/mm Hg (Fig. 5d).

Because the SAKC activity recorded on the blebs showed obvious adaptation/inactivation during stimulation (Fig. 5c), both the peak and steady activities of the bleb SAKC were calculated. In steady state before cyto-B, $NP_o = 0.004e^{0.06x}$ ($R^2 = 0.97$, $n = 5$), and after 20-min exposure to cyto-B $NP_o = 0.02e^{0.08x}$ ($R^2 = 0.99$, $n = 5$). In the bleb membrane, peak NP_o was fitted by $0.16e^{0.08x}$ ($R^2 = 0.87$, $n = 4$) and in the steady state by $0.10e^{0.04x}$ ($R^2 = 0.98$, $n = 5$). These data are shown in the semilog plot of NP_o in Fig. 5d where the intercept (A) is the background activity and the slope (k) is the slope sensitivity. Three plots for control and cyto-treated cells and the peak NP_o of the bleb were nearly parallel, differing mainly in the resting activity, although the determination coefficient ($R^2 = 0.87$) for the peak NP_o of the bleb was a small deviation from 1, suggesting that the mechanical properties of the bleb patch differed to some extent from those of control. The consistency of the slopes for the three conditions implies that the slope was not sensitive to cyto-B and hypotonic treatment, and the conformational change of the channel was similar in each case. The drop in slope sensitivity of SAKCs in steady phase probably reflects a kinetic effect in which more than one rate constant is tension-sensitive.

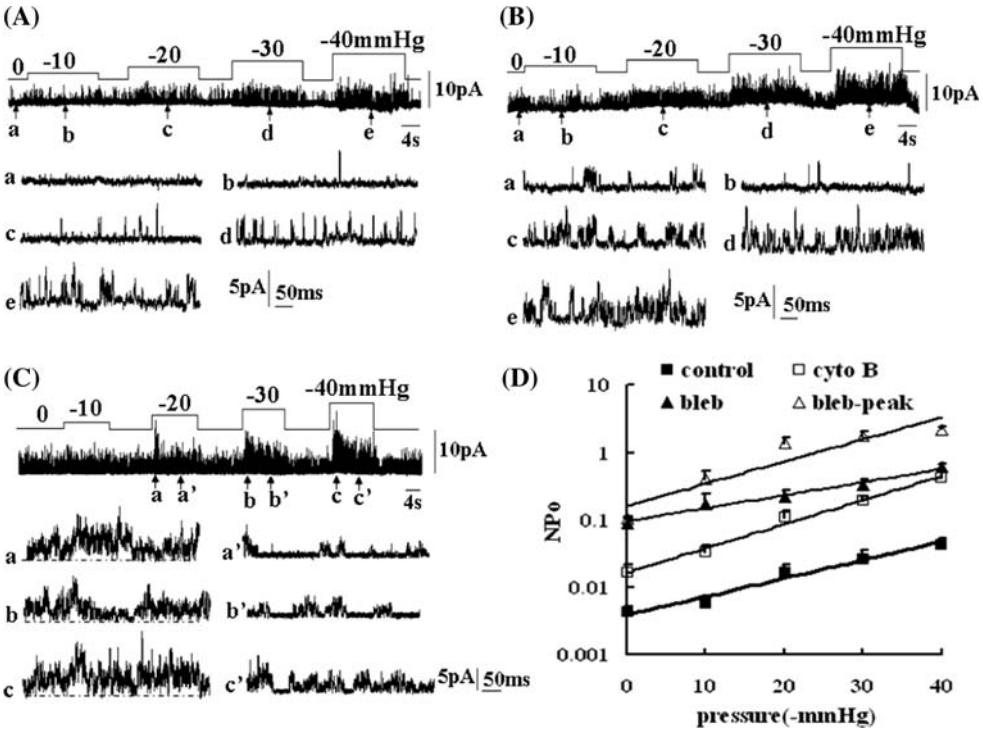

Fig. 5 Pressure-dependent activation of SAKCs in three different mechanical microenvironments. **a** and **b** were recorded from the same cell-attached patch, holding at +40 m*V* in symmetrical 140 mM K^+ aspartate before and after applying cyto-B (20 μM) in the bath. **c** was recorded in bleb membrane. *Lower sections* of **a–c** are expanded traces chosen at the time with the corresponding *arrows* in the *upper section*. In **c**, *a–c* show the channel activity at the peak phase, while *a'–c'* are in the steady state. **d** Relationship of SAKC open probability (NP_o) and suction. ■ and □, the same patches ($n = 5$) before and after treatment with cyto-B; Δ and ▲, NP_o in the peak ($n = 4$) and steady ($n = 5$) phases of bleb patches

Discussion

The Identity of SAKCs in the Control Membrane and Bleb

Normal and bleb membrane currents had similar conductance and *I–V* relations, reversing at 0 m*V* in symmetrical K^+ condition with similar responses to stretch, AA and acidity. Taken together, these characteristics suggest SACs in both types of patches were the same and K^+-selective. TREK-1 is known to be expressed in rat cardiac myocytes (Tan et al. 2002; Terrenoire et al. 2001; Xian Tao et al. 2006). Several types of potassium channels in the cardiac myocyte, such as TREK-1, ATP-sensitive and ACh-activated channels, have been reported to respond to mechanical stimulation (Patel et al. 2001; Pleumsamran and Kim 1995; Van Wagoner 1993); but the SAKCs identified in our data were not K_{ATP} and K_{ACh}. TREK-1 opens over the entire range of physiological voltages; is also activated by stretch, AA and acid; and is insensitive to intracellular Ca^{2+} and classical K^+-channel blockers (Patel et al. 2001). Our results are consistent with these reports.

As early as 1995, three types of K^+ channels in cultured rat neuronal cells were reported with *I–V* relationships that were slightly outwardly rectifying, inwardly rectifying and linear, with single-channel slope conductances at +60 m*V* of 143, 45 and 52 pS, respectively. All three types were activated by AA, low pH and negative pressure (Kim et al. 1995). In another report, TREK-1-like 56-pS currents from cultured mouse striatal neurons showed outward rectification in physiological solutions and were nearly linear in symmetrical K^+ (Chemin et al. 2005, see their Fig. 1a). This diversity also exists in cardiac myocytes. Terrenoire et al. (2001) reported a type of TREK-1-like channel with outward rectification and a conductance of 41 pS at +50 m*V* in rat atrial cells, while Tan et al. (2002) reported a TREK-1-like channel in rat ventricular myocytes with 111 pS and a linear *I–V* relation. Subsequently, it was reported that TREK-1-like channels in rat ventricular muscle manifested both a large-conductance state (132 pS at positive potential) with outward rectification and a low-conductance state (41 pS at positive potential) with weak inward rectification (Joon Kim and Earm 2006; Xian Tao et al. 2006). Furthermore, TREK-1-like channels showed a low-conductance mode in the majority of patches (Joon Kim and Earm 2006; Xian Tao et al. 2006), which was close to that in the present study. We have never recorded large-conductance TREK-1-like channels, so the atrial SAKCs in the present study appear to be a subset of TREK-1-like channel states.

The Mechanical Microenvironment of Blebs

The cortical cytoskeleton is a complicated protein network that connects the deeper parts of the sarcomere with the sarcolemma. The costamere is a hub of mechanical and chemical signals connecting the extracellular matrix, the sarcolemma and the Z-disk. As a main part of the cortical

cytoskeleton, the costamere with integral proteins comprises three groups of protein complexes: spectrin/ankyrin/transporter (and some other types of channels), dystrophin/dystroglycan and vinculin/talin/α-actinin/integrin. All three groups connect to the Z-disk through F-actin filaments (Rybakova et al. 2000). This linkage may protect the sarcolemma from disengaging from the Z-disk during contraction. However, it is still not known whether cardiac SACs physically connect to the actin skeleton.

In our blebbed cardiac myocytes, the bleb size was 20–50 μm covering 10–20 adjacent sarcomeres. There was no F-actin visible beneath the bleb membrane. The bleb morphology under electron microscopy was the same as that described by Collins et al. (1992) with a smooth membranous structure and no caveoli (Fig. 1). The hypotonically induced bleb was similar to the bleb induced hypertonically in oocytes; both were smooth with no F-actin skeleton and had functional SACs. SAKC activity in the hypotonically induced bleb of cardiac myocytes appears similar to SACs in the oocytes and the liposomes. However, the background membrane tension may be quite different. Because our blebs were induced by swelling and gradually enlarged, there might be more background membrane tension in the bleb membrane than in the hypertonically induced oocyte bleb and the liposome.

During mechanical stimulation, suction on the patch is balanced by wall tension of the gigaseal and stresses in the underlying cytoskeleton. Accordingly, when the cortical F-actin was disrupted or removed, the tension shared by the lipid membrane would increase. The high background activity of SAKC in blebs is consistent with this model. The hypotonically induced bleb presumably has the same properties as the hypertonically induced bleb with native lipid components and normal channel orientation (Zhang et al. 2000). However, the former may be a simplified model more useful for studying cardiac SAKC gating because the bleb membrane is simpler than the sarcolemma patch dynamics and, hence, SAKC gating probably changes.

Gating Mechanism of SAKCs in Cardiac Myocytes

In the bilayer model of SAC gating, the cortical skeleton is parallel with the bilayer and assumed to protect the lipid membrane as well as the inlaid SACs against excess stress. The key data proving that membrane lipids can directly transmit force to SAC were provided by studies of bacterial SACs reconstituted into liposomes (Jeon and Voth 2008; Sukharev 2002; Sukharev et al. 1994).

Additional indirect evidence for eukaryotes came from a study of SACs in hypertonically induced oocyte blebs (Maroto et al. 2005; Zhang et al. 2000), where SACs in the bleb retained mechanosensitivity. The C terminus of TREK-1 has a positively charged cluster around E306 that appears to be responsible for channel–phospholipid interactions and acid sensing, and these lipid interactions suggest that TREK-1 is activated by force coupled via the lipid bilayer (Chemin et al. 2005; Honore et al. 2002). Furthermore, pressure activation of TRAAK, a TREK-related channel, has also been demonstrated in hypertonically induced oocyte blebs (Honore et al. 2006). However, the ultimate evidence that mechanical gating of TREK-1 is mediated directly by the bilayer will require reconstitution in artificial lipids.

We did not analyze the SAKC transient kinetics since the manually controlled mechanical stimulations were too slow. However, we noticed that SAKC in some blebs had a time-dependent decrease in current that could be due to channel inactivation or relaxation of the local stress, i.e., adaptation (Figs. 2b and 5c). The time course was similar to that in the previous study of atrial cells (Niu and Sachs 2003) but much slower than the 100-ms "relaxation" time reported for TREK-1 by Honore et al. (2006). Their tests of inactivation suggested it was not adaptation.

NP_o of SAKCs at rest and during suction was the highest in the blebs and the lowest in control cells (Fig. 5d). The variation of the intercepts in Fig. 5d implies that a variable fraction of gigaseal tension is transferred to the channels, probably by the sharing of stress with the cytoskeleton. The slope sensitivity of SAKCs to pressure that reflects the change in dimensions of the channel was insensitive to treatment with cytochalasin or blebbing. The evidence from nonselective SACs of bacteria (Martinac 2004; Martinac et al. 1990; Sukharev 2002; Sukharev et al. 1994), cation-selective SACs (Zhang et al. 2000) and TRAAK (Honore et al. 2006) expressed in oocytes, as well as SAKCs of cardiac myocytes, suggests that the bilayer model of SAC mechanosensitivity is quite general.

Acknowledgements This study was supported by grants from National Natural Science Foundation of China (30570663), Beijing Education Committee (KM200510025001), Beijing Natural Science Foundation (7052012) and the NIH (to F. S.). The authors kindly thank Prof. Tai-Feng Liu for revising the manuscript and Prof. Zhen-Wei Liu for help in single-channel data analysis.

References

Akinlaja J, Sachs F (1998) The breakdown of cell membranes by electrical and mechanical stress. Biophys J 75:247–254

Baumgarten CM, Clemo HF (2003) Swelling-activated chloride channels in cardiac physiology and pathophysiology. Prog Biophys Mol Biol 82:25–42

Casadei B, Sears CE (2003) Nitric-oxide-mediated regulation of cardiac contractility and stretch responses. Prog Biophys Mol Biol 82:67–80

Chemin J, Patel AJ, Duprat F, Lauritzen I, Lazdunski M, Honore E (2005) A phospholipid sensor controls mechanogating of the K^+ channel TREK-1. EMBO J 24:44–53

Christensen A, Corey D (2007) TRP channels in mechanosensation: direct or indirect activation? Nat Rev Neurosci 8:510–521

Collins A, Somlyo AV, Hilgemann DW (1992) The giant cardiac membrane patch method: stimulation of outward Na^+–Ca^{2+} exchange current by MgATP. J Physiol 454:27–57

Corey D (2003) Sensory transduction in the ear. J Cell Sci 116:1–3

Corey DP, Hudspeth AJ (1983) Kinetics of the receptor current in bullfrog saccular hair cells. J Neurosci 3:962–967

Franz MR, Cima R, Wang D, Profitt D, Kurz R (1992) Electrophysiological effects of myocardial stretch and mechanical determinants of stretch-activated arrhythmias. Circ 86:968–978

Furukawa T, Yamane T, Terai T, Katayama Y, Hiraoka M (1996) Functional linkage of the cardiac ATP-sensitive K^+ channel to the actin cytoskeleton. Pfluegers Ach 431:504–512

Gottlieb P, Folgering J, Maroto R, Raso A, Wood T, Kurosky A, Bowman C, Bichet D, Patel A, Sachs F, Martinac B, Hamill O, Honoré E (2008) Revisiting TRPC1 and TRPC6 mechanosensitivity. Pfluegers Arch 455:1097–1103

Hamill OP (2006) Twenty odd years of stretch-sensitive channels. Pfluegers Arch 453:333–351

Hamill OP, McBride DW Jr (1992) Rapid adaptation of single mechanosensitive channels in *Xenopus* oocytes. Proc Natl Acad Sci USA 89:7462–7466

Hamill OP, McBride DW Jr (1997) Induced membrane hypo/hypermechanosensitivity: a limitation of patch-clamp recording. Annu Rev Physiol 59:621–631

Hilgemann DW (1989) Giant excised cardiac sarcolemmal membrane patches: sodium and sodium–calcium exchange currents. Pfluegers Arch 415:247–249

Honore E, Maingret F, Lazdunski M, Patel AJ (2002) An intracellular proton sensor commands lipid- and mechano-gating of the K^+ channel TREK-1. EMBO J 21:2968–2976

Honore E, Patel AJ, Chemin J, Suchyna T, Sachs F (2006) Desensitization of mechano-gated K_{2P} channels. Proc Natl Acad Sci USA 103:6859–6864

Hu H, Sachs F (1997) Stretch-activated ion channels in the heart. J Mol Cell Cardiol 29:1511–1523

Jeon J, Voth G (2008) Gating of the mechanosensitive channel protein MscL: the interplay of membrane and protein. Biophys J 94:3497–3511

Joon Kim S, Earm YE (2006) Dual conductance mode of the TREK-1 channel: a hidden track to mechanoelectric regulation in the heart? Cardiovasc Res 69:13–14

Kim D, Sladek CD, Aguado-Velasco C, Mathiasen JR (1995) Arachidonic acid activation of a new family of K^+ channels in cultured rat neuronal cells. J Physiol 484:643–660

Lesage F, Lazdunski M (2000) Molecular and functional properties of two-pore-domain potassium channels. Am J Physiol 279:F793–F801

Lopes C, Rohács T, Czirják G, Balla T, Enyedi P, Logothetis D (2005) PIP_2 hydrolysis underlies agonist-induced inhibition and regulates voltage gating of two-pore domain K^+ channels. J Physiol 564:117–129

Maingret F, Fosset M, Lesage F, Lazdunski M, Honoré E (1999) TRAAK is a mammalian neuronal mechano-gated K^+ channel. J Biol Chem 274:1381–1387

Maroto R, Raso A, Wood TG, Kurosky A, Martinac B, Hamill OP (2005) TRPC1 forms the stretch-activated cation channel in vertebrate cells. Nat Cell Biol 7:179–185

Martinac B (2004) Mechanosensitive ion channels: molecules of mechanotransduction. J Cell Sci 117:2449–2460

Martinac B, Adler J, Kung C (1990) Mechanosensitive ion channels of *E.* coli activated by amphipaths. Nature 348:261–263

Niu W, Sachs F (2003) Dynamic properties of stretch-activated K^+ channels in adult rat atrial myocytes. Prog Biophys Mol Biol 82:121–135

Patel AJ, Lazdunski M, Honore E (2001) Lipid and mechano-gated 2P domain K^+ channels. Curr Opin Cell Biol 13:422–427

Pleumsamran A, Kim D (1995) Membrane stretch augments the cardiac muscarinic K^+ channel activity. J Membr Biol 148:287–297

Rybakova IN, Patel JR, Ervasti JM (2000) The dystrophin complex forms a mechanically strong link between the sarcolemma and costameric actin. J Cell Biol 150:1209–1214

Sukharev S (2002) Purification of the small mechanosensitive channel of *Escherichia coli* (MscS): the subunit structure, conduction, and gating characteristics in liposomes. Biophys J 83:290–298

Sukharev SI, Blount P, Martinac B, Blattner FR, Kung C (1994) A large-conductance mechanosensitive channel in *E.* coli encoded by mscL alone. Nature 368:265–268

Tan JHC, Liu W, Saint DA (2002) Trek-like potassium channels in rat cardiac ventricular myocytes are activated by intracellular ATP. J Membr Biol 185:201–207

Terrenoire C, Lauritzen I, Lesage F, Romey G, Lazdunski M (2001) A TREK-1-like potassium channel in atrial cells inhibited by beta-adrenergic stimulation and activated by volatile anesthetics. Circ Res 89:336–342

Van Wagoner DR (1993) Mechanosensitive gating of atrial ATP-sensitive potassium channels. Circ Res 72:973–983

Wei H, Huang H, Wang W, Zhang Z, Fu X, Liu P, Niu W (2006) A ventricular pressure-clamping system for the study of mechano-electrical feedback. Sheng Li Xue Bao 58:606–610

Xian Tao L, Dyachenko V, Zuzarte M, Putzke C, Preisig-Muller R, Isenberg G, Daut J (2006) The stretch-activated potassium channel TREK-1 in rat cardiac ventricular muscle. Cardiovasc Res 69:86–97

Yamazaki T, Komuro I, Yazaki Y (1996) Molecular aspects of mechanical stress-induced cardiac hypertrophy. Mol Cell Biochem 163(164):197–201

Zhang Y, Gao F, Popov VL, Wen JW, Hamill OP (2000) Mechanically gated channel activity in cytoskeleton-deficient plasma membrane blebs and vesicles from *Xenopus* oocytes. J Physiol 523:117–130